RECONSTRUCTION OF PORE-SPACE IMAGES USING MICROTOMOGRAPHY AND MULTIPLE-POINT STATISTICS

HIROSHI OKABE [1, 2] AND MARTIN J. BLUNT [2]

[1] *Japan Oil, Gas and Metals National Corporation, 1-2-2 Hamada, Mihama-ku, Chiba, 261-0025, Japan*

[2] *Department of Earth Science and Engineering, Imperial College London, SW7 2AZ, United Kingdom*

ABSTRACT

Quantitative prediction of petrophysical properties for reservoir rocks frequently employs representative microscopic models of the pore space as input. Recently digital imaging techniques such as microtomography have been used to provide void space images at the resolution of a few microns. However, this resolution may be insufficient to capture some smaller structures, particularly in carbonates. An emerging destructive focused ion beam method can provide better resolution but only on very small samples. Two-dimensional (2D) thin sections, in contrast, are easily available and they can image micro-porosity. However, they do not directly capture the three-dimensional (3D) pore space. We propose an integrated approach to combine different types of image to reconstruct porous media. In order to generate geologically realistic pore space images with appropriate connectivity, particularly for carbonate rocks, relatively low resolution microtomography and higher resolution images from thin-sections are used. 2D thin-sections provide multiple-point statistics (MPS), which describe the statistical relation between multiple spatial locations and their statistics can be used to generate 3D images at higher resolution. The reconstruction using multiple-point statistics allows the connectivity of the void space to be reproduced accurately. The statistically reconstructed images are then combined with the images measured by the microtomography to generate a realistic pore structure since some 2D thin-sections may miss macro-porosity due to their size. The integrated method is tested on carbonates for which 3D images of larger vug porosity are captured, while 2D thin sections accurately characterize small-scale structure. The integrated images have permeabilities computed using the lattice-Boltzmann method (LBM) that are similar to laboratory-measured values, which indicates that the proposed method is both practical and realistic.

1. INTRODUCTION

The reconstruction of porous media is of great interest in a wide variety of fields, including earth science and engineering, biology and medicine, since the geometry and topology of the reconstructed structure are critical characteristics to determine physical and mechanical properties. Several methods have been proposed to generate 3D pore space images. A series of 2D sections can be stacked to form a 3D image. However, this operation is limited by the impossibility of preparing cross sections with a spacing of less than about

10μm. Recently, the use of a focused ion beam technique [*Tomutsa and Radmilovic*, 2003] overcomes the problem of resolution and allows sub-micron images to be constructed. Non-destructive X-ray computed microtomography [*Spanne, et al.*, 1994] is another approach to image a 3D pore space directly at resolutions of around a micron. The resolution of the imaging technique is, however, not sufficient to capture sub-micron size pores that are abundant in carbonates. The sub-micron structures of real rocks have been studied using laser scanning confocal microscopy [*Fredrich*, 1999]; however, it also has limited ability to penetrate solid materials. In the absence of higher resolution 3D images, reconstructions from readily available 2D microscopic images such as scanning electron microscopy (SEM) are the only viable alternative.

2D high-resolution images provide important geometrical properties such as the porosity, ϕ, and typical pore-space patterns. Based on the information extracted from 2D images, one approach is to reconstruct the porous medium by modeling the geological process by which it was made [*Bakke and Øren*, 1997; *Bryant and Blunt*, 1992]. Although this process-based reconstruction is general and can reproduce the long-range void connectivity, there are many systems for which the process-based reconstruction is very difficult to apply. For instance, for many carbonates it would be complex to use a process-based method that mimics the geological history involving the sedimentation of irregular shapes followed by significant compaction, dissolution and reaction [*Lucia*, 1999]. In these cases it is necessary to find another approach to generate a pore space representation. Traditionally two-point statistics has been used; however, this often fails to reproduce the long-range connectivity of the pores, especially for low porosity media. We have reconstructed geologically realistic pore space structures using a multiple-point statistical technique [*Okabe and Blunt*, 2004], which uses higher order statistics [*Caers*, 2001; *Strebelle, et al.*, 2003]. In our previous work, we studied sandstones and carbonates and showed that the long-range connectivity of the pore space was better reproduced than when using two-point statistics, while the numerically predicted permeabilities of the images were in good agreement with measured values. Since the method is suitable for any material, including those with sub-micron structures, we apply the method to a vuggy carbonate rock. This is a particular challenge, since the macro-pores are not directly connected and an accurate assessment of permeability requires an estimate of the size and connectivity of sub-micron pores between the vugs. Statistically reconstructed 3D pore structures are combined with directly measured images. To validate these integrated images of micro- and macro-pores, the lattice-Boltzmann method is used to predict permeability.

2. MULTIPLE-POINT STATISTICS RECONSTRUCTION

Multiple-point statistics (MPS) cannot be inferred from sparse data; their inference requires a densely and regularly sampled training image describing the geometries expected to exist in the real structure. Microscope images at the pore scale can be used as training images. In our application only two phases are used – void and solid phase. The method to reconstruct a 3D image from 2D information is an extended version of the multiple-point statistics approach that was developed for the field scale [*Caers*, 2001; *Srivastava*, 1992; *Strebelle, et al.*, 2003]. We assume isotropy in orthogonal directions to generate a 3D image using MPS measured on a 2D plane. We assume that only a single 2D plane is available to reconstruct 3D images in this study. The training image and the template to capture patterns (multiple-point

statistics) used are shown in FIGURE 1. The measured statistics are rotated by 90 degrees, which allows us to generate a 3D structure based on a single training plane. Since the MPS method is well-established in geostatistics, we will not repeat the standard procedure to generate 2D images from 2D training images in detail. The procedure consists of three steps: (1) extracting MPS from the training image; (2) probability calculation on each orthogonal plane using conditioning data; and (3) pattern reproduction using the probability weighted by the number of conditioning data on each plane.

Here we explain how to generate a 3D image using a 2D training image. After extracting every possible pattern in the training image, every unit voxel in a 3D domain is visited once randomly. At every voxel, in order to assign void or solid phase, three principal orthogonal planes, XY, XZ and YZ intersecting the designated voxel are used to find conditioning data on these planes one by one. Consideration of the orthogonal planes is important to reproduce proper connectivity. The process, which is equivalent to the running of a 2D MPS simulation for single plane, estimates each probability of the phase at the voxel on the different planes. Then the three measured probabilities are linearly weighted by the number of conditioning data on each plane to obtain a single probability on the voxel. Finally, the phase at the voxel is assigned based on this weighted probability to generate a 3D image assuming isotropy in orthogonal planes. If anisotropy is expected to exist in 3D, multi-orientation thin sections can be used as training images. There is less conditioning data during the initial stage of the reproduction. In this case, the porosity value can be used as the probability. Further details of the procedure can be found in [*Okabe and Blunt*, 2004].

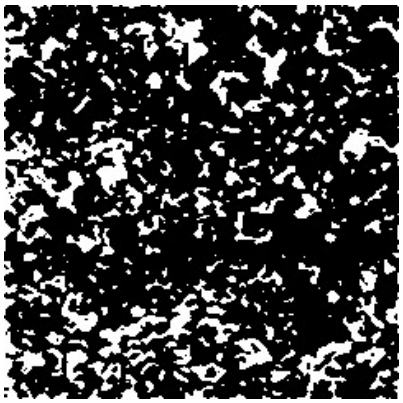

(A) Training image (B) Template

FIGURE 1. (A) An example of a training image taken from a 2D thin-section of a carbonate rock with a porosity of 0.213 (240^2 pixels). The training image is chosen to avoid macro-pores. The void space is shown white and the solid black. The resolution of the image is 0.709μm/pixel. (B) A 9 × 9 template used to capture multiple-point statistics. The training image is scanned and each occurrence of any possible patterns of void space and solid is recorded. We also use a succession of larger templates using a form of multigrid simulation [*Strebelle, et al.*, 2003].

3. LATTICE-BOLTZMANN METHOD FOR PERMEABILITY

The lattice-Boltzmann method (LBM) provides a good approximation to solutions of the Navier-Stokes equations using a parallel and efficient algorithm that readily accommodates

complex boundaries, as encountered in porous media [*Buckles, et al.*, 1994]. Therefore, the LBM, particularly LBGK (lattice-Bhatnagar-Gross-Krook) model, described in equation (1) is used to calculate single-phase permeability to examine the reconstructed structure quantitatively [*Chen and Doolen*, 1998]. A three-dimensional nineteen-velocity model, D3Q19, that includes a rest vector is used. The bounce-back scheme at walls is used to obtain no-slip velocity conditions and the flow field is computed using periodic boundary conditions.

$$f_i\left(\mathbf{x}+\mathbf{e}_i, t+1\right) - f_i\left(\mathbf{x}, t\right) = -\frac{1}{\tau}\left[f_i\left(\mathbf{x}, t\right) - f_i^{(eq)}\left(\mathbf{x}, t\right)\right] \quad (1)$$

where $f_i\left(\mathbf{x}, t\right)$ is the particle distribution function at space **x** and time *t* along the *i*-th direction (*i*=0,1,2, …, 18 in our case). $\mathbf{e}_i$ is the local particle velocity and τ is the single time relaxation parameter. $f_i^{(eq)}$ is the local equilibrium state depending on the local density and velocity.

4. COMBINING MPS RECONSTRUCTED IMAGES WITH MICROTOMOGRAPHY

Digital imaging technique of microtomography has been used to provide void space information at a resolution of a few microns. However, the images may not be sufficient to capture some smaller structures beyond the resolution of the technique, particularly in carbonates. We propose an integrated method in order to fill the gap between macro-pores measured by micro computed tomography (micro-CT) and to restore the original connectivity in the rock. To validate integrated images with micro- and macro-pores in terms of the transport properties, the lattice-Boltzmann method described above is used. The LBM, however, is limited by the size of the input structure due to the computational time. Therefore, permeability can only be computed on relatively small images.

4.1 Microtomography of the rock sample.

A Cretaceous carbonate rock sample used in the study mainly consists of algal bioclastic peloidal packstone/grainstone and has an average porosity of 0.304 and air permeability of 32.9mD measured on a 1.5 inch diameter core plug. A microtomography image, FIGURE 2(A), is partitioned into void and solid, FIGURE 2(B) to yield an image with a porosity of approximately 0.104. Smaller parts of the binalized image are then combined with statistically reconstructed images using a training image shown in FIGURE 1(A).

4.2 Combining macro-pores with micro-pores

While macro-porosity is provided by the microtomography explained above, micro-porosity at the sub-micron scale can only be reproduced by statistical reconstruction. A training image, FIGURE 1(A), is chosen to capture only the pattern of micro-pores since macro-pores have been identified by micro-CT. However, macro-pores are seen near the training image taken. In order to restore a well connected pore structure, macro-pores have to be linked by micro-pores. Two different types of pore are separately reconstructed by direct imaging and statistical reconstruction. Macro-pores are superimposed on the micro-pores as shown in FIGURE 3. As the images have different resolutions, the scale of the measured microtomographic image is adjusted to that of statistical reconstruction. The resolution of the direct image is eight times larger than that of the MPS reconstructed image in the study;

therefore, the image reconstructed by micro-CT is scaled to match the resolution of the statistically reconstructed image.

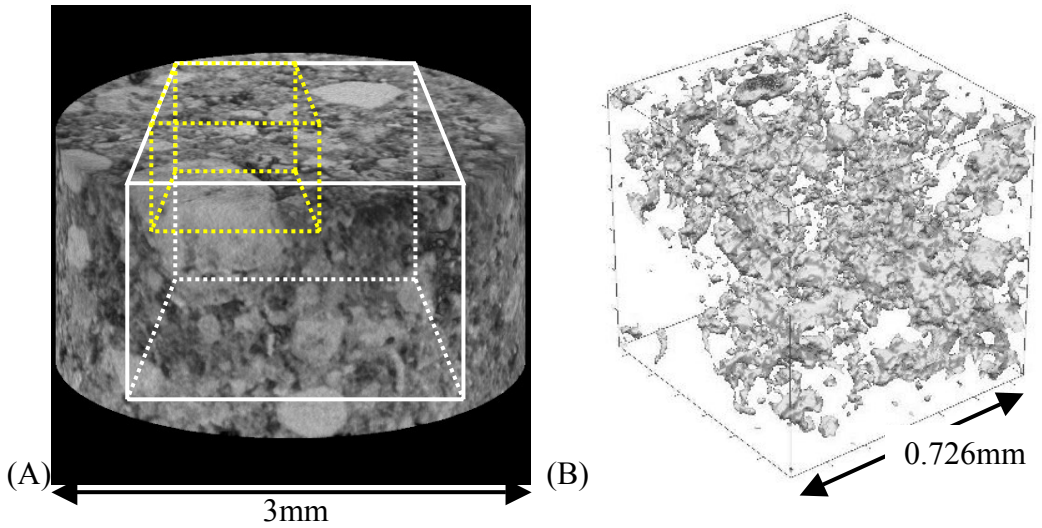

FIGURE 2. (A) A larger grey scale image and (B) a smaller binalized image of the microtomography of the sample. The image (A) has a macro-porosity of 0.106 identified by micro-CT with a resolution of 5.67μm/voxel and the binalized image (B) extracted from the image (A) has a porosity of 0.104.

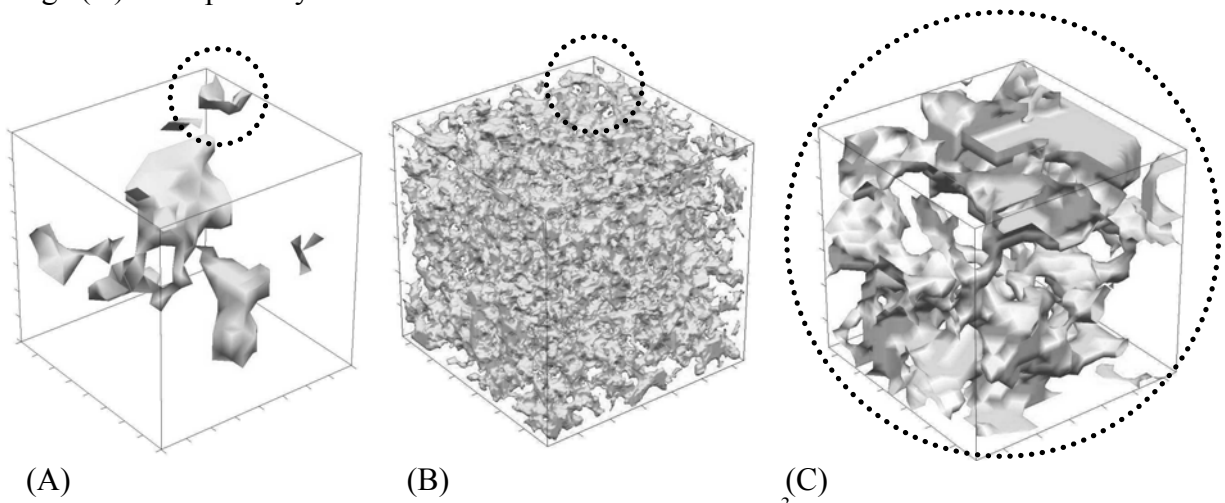

FIGURE 3. Smaller parts of reconstructed images (size=128^3, 0.709μm/voxel). (A) A part of the microtomography image with macro-pores that are not well connected (porosity, ϕ =0.0991), (B) one realization of a reconstructed image using MPS (ϕ =0.221) and (C) a smaller combined image of (A) and (B) with the subset of the volume marked by the dotted circle (size=32^3, ϕ =0.299).

5. FLOW PROPERTIES

Permeabilities of the reconstructed microstructures are computed using the lattice-Boltzmann method (LBM) described before. Since only sections of the original images are used to validate the proposed method, structures using different parts of the microtomography

are tested. The statistically reconstructed images have little variability in terms of vertical permeability; k_z estimated by the LBM (k_z =5.3-8.1mD) because they are all based on a relatively homogeneous training image. However, the different subsets of microtomography, as shown in FIGURE 4, introduce different porosity and connectivity characteristics.

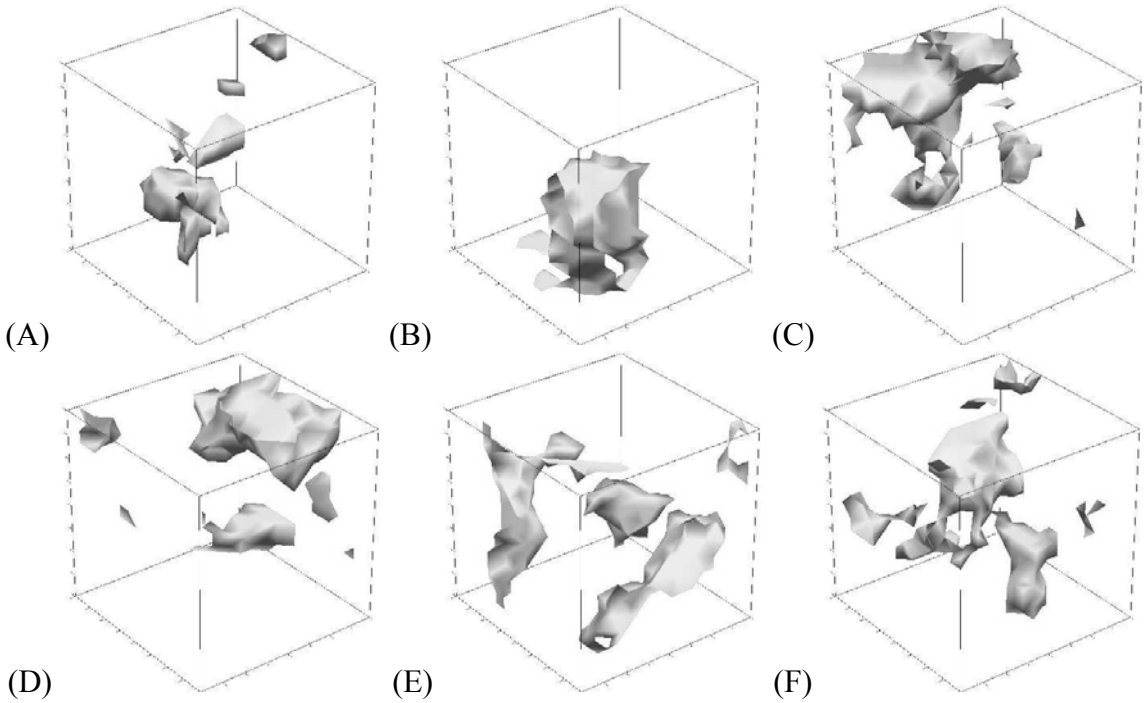

FIGURE 4. Extracted subsets (size=128^3) from the 3D microtomography of macro-pores with different porosity values. (A) ϕ=0.05, (B) ϕ=0.075, (C)-(F) have almost same macro-porosity, ϕ =0.10, but the locations of these subsets taken in the measured microtomography are different.

The computed permeabilities of the combined microstructures with total porosities varied from 0.25 to 0.30 are listed in TABLE 1 and the correlation between macro-porosities and computed permeabilities is shown in FIGURE 5. All cases use the same 10 realizations reconstructed using MPS with porosities around 0.22. Therefore, the combined images with the different macro-porosities ranging from 0.05 to 0.10, have different total porosities. Although four cases have similar porosity values of 0.10, the distributions of macro-pores as shown in FIGURE 4 (C) to (F) are different. The computed permeabilities as a consequence vary from 17.2 to 53.7mD with an average of 33.2mD.

Although the size of combined images for this carbonate rock (128^3 at 0.709μm/voxel giving a total size of around 90 μm) might be too small to compare with the experimental properties, the average of the computed permeabilities is in good agreement with the measured value for the core and it is also good considering the large size difference between reconstructed images and the experimental sample. Larger images can be generated using the proposed method although it is not practical to calculate their permeabilities using the LBM. The method is, however, able to produce geologically realistic images with micro- and macro-

pores with appropriate connectivities. Therefore, it can be used to generate pore network structures to predict single- and multi-phase flow properties.

TABLE 1. The computed permeabilities of the combined microstructures using multiple-point statistics reconstructions with porosities of approximately 0.22 and the different subsets of microtomography with porosities ranging from 0.05 to 0.10.

Combined image	Averaged porosity		Averaged permeability
	macro-porosity	Total	k_z (mD)
Reconstructions using FIGURE 4(A)	0.05	0.259	10.7
Reconstructions using FIGURE 4(B)	0.075	0.279	22.2
Reconstructions using FIGURE 4(C)	0.100	0.298	36.6
Reconstructions using FIGURE 4(D)	0.102	0.299	17.2
Reconstructions using FIGURE 4(E)	0.102	0.299	53.7
Reconstructions using FIGURE 4(F)	0.099	0.298	24.6

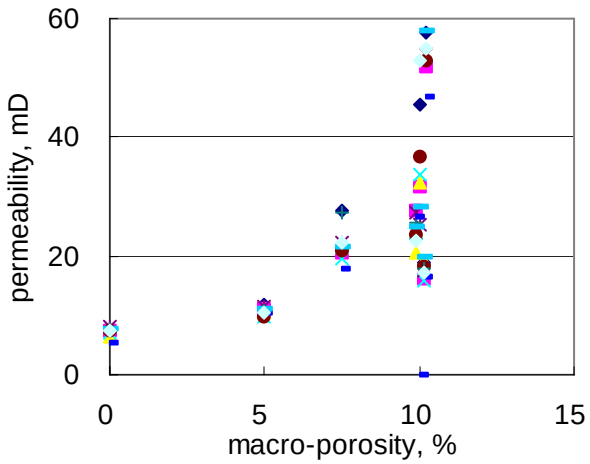

FIGURE 5. Variation of computed permeabilities in combined images with different macro-porosities. As the macro-porosity is increased, the range of permeabilities becomes large for these small reconstructed images due to heterogeneous distributions of macro-pores. The range of permeability will be reduced as the size of the image is increased.

6. CONCLUSIONS

Multiple-point statistics reconstruction using a 2D thin section to generate 3D pore-space representations of rocks has been used to generate micro-pores while larger macro-pores are identified by microtomography. These two different methods focused on different scales are integrated to reconstruct geologically realistic pore structures with appropriate connectivities. The microstructures of a carbonate rock were reconstructed and their permeabilities simulated by the lattice-Boltzmann method were compared with the experimental data. The predicted permeabilities were in good agreement with the experiment value although the size of reconstructed images is smaller than a conventional laboratory sample. A combination of a statistical reconstruction and a direct imaging technique successfully reproduced realistic microstructures. Larger combined images were not tested using the method since it was

unpractical to calculate their permeabilities using the lattice-Boltzmann method. However, the method could produce geologically realistic images with micro- and macro-pores with good connectivities, which would be directly used to generate pore network structures in order to predict single- and multi-phase flow properties using pore-scale modeling [*Blunt, et al.*, 2002].

7. ACKNOWLEDGEMENTS

The authors would like to express their gratitude to Japan Oil, Gas and Metals National Corporation (JOGMEC).

REFERENCES

Bakke, S., and P. E. Øren (1997), 3-D pore-scale modelling of sandstones and flow simulations in the pore networks, *SPE Journal*, *2*, 136-149.

Blunt, M. J., et al. (2002), Detailed physics, predictive capabilities and macroscopic consequences for pore-network models of multiphase flow, *Advances in Water Resources*, *25*, 1069-1089.

Bryant, S., and M. J. Blunt (1992), Prediction of relative permeability in simple porous-media, *Physical Review A*, *46*, 2004-2011.

Buckles, J. J., et al. (1994), Toward improved prediction of reservoir flow performance - simulating oil and water flows at the pore scale, *Los Alamos Science*, *22*, 112-120.

Caers, J. (2001), Geostatistical reservoir modelling using statistical pattern recognition, *Journal of Petroleum Science and Engineering*, *29*, 177-188.

Chen, S., and G. D. Doolen (1998), Lattice Boltzmann method for fluid flows, *Annu Rev Fluid Mech*, *30*, 329-364.

Fredrich, J. T. (1999), 3D imaging of porous media using laser scanning confocal microscopy with application to microscale transport processes, *Physics and Chemistry of the Earth Part A-Solid Earth and Geodesy*, *24*, 551-561.

Lucia, F. J. (1999), *Carbonate reservoir characterization*, Springer, Berlin.

Okabe, H., and M. J. Blunt (2004), Prediction of permeability for porous media reconstructed using multiple-point statistics, *Physical Review E*, *70*, art. no.-066135.

Spanne, P., et al. (1994), Synchrotron computed microtomography of porous-media - topology and transports, *Physical Review Letters*, *73*, 2001-2004.

Srivastava, M. (1992), Iterative methods for spatial simulation, Stanford, CA.

Strebelle, S., et al. (2003), Modeling of a deepwater turbidite reservoir conditional to seismic data using principal component analysis and multiple-point geostatistics, *SPE Journal*, *8*, 227-235.

Tomutsa, L., and V. Radmilovic (2003), Focussed ion beam assisted three-dimensional rock imaging at submicron-scale, paper presented at International Symposium of the Society of Core Analysts, Pau, France.